Integral Equation Formulations For Scattering Problems

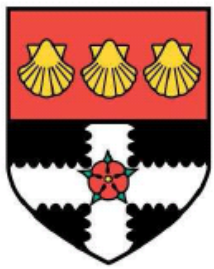

UNIVERSITY OF READING
Department of Mathematics

Charlotta Jasmine Howarth

August 2009

This dissertation is submitted to the Department of Mathematics in partial fulfilment of the requirement for the degree of Master of Science.

Abstract

In this thesis we are concerned with the study of scattering of acoustic waves generated by the interaction of an incident wave with an object producing reflected and diffracted waves; we study the case of a square in detail. We look at how the wave scattering problem based upon the Helmholtz equation can be reformulated to a lesser dimension size using integral equation formulations. This process may give rise to non unique solutions not inherent to the original problem. To investigate this, we consider two Boundary Element Methods that can be used to find an approximate solution numerically. The first, a standard collocation method, illustrates how easily spurious solutions are found. The second, a hybrid Galerkin BEM proposed by Langdon and Chandler-Wilde, illustrates how careful consideration of the desired solution when designing a numerical method can avoid these spurious solutions whilst saving on computational time.

Acknowledgements

I would like to thank firstly Dr. Stephen Langdon who supervised this project, for all the time, support, and knowledge he has given me, and for making this such an enjoyable project. All of the lecturers that have been helpful to me this year and taught me so much, a big thank-you goes to you guys. I would also like to thank all the postgraduate students of the Mathematics Department for their friendship, in particular to my fellow coursemates for the support, laughter, cups of tea, and pizza over this stressful year, and for the times of insanity in the computer room. Finally, I would like to recognise the financial support provided by the ESPRC studentship, without which I couldn't have persued the studies I enjoy so much.

Declaration

I confirm that this is my own work, and the use of all material from other sources has been properly and fully acknowledged.

Signed .....

Contents

Chapter 1

Introduction

1.1 Motivation

Scattering problems for acoustic and electromagnetic waves have been the subject of much theoretical and numerical study. There are many applications in the fields of physics, engineering, and geology, including radar and sonar, medical imaging, and geophysical exploration. Direct scattering problems are those which aim to find the scattered field produced by the interaction of a known incident wave with an object, whereas the inverse scattering problem is that of trying to determine the nature of the object or domain of definition, based upon the behaviour of the scattered wave. These problems are often not solvable analytically, and so various numerical techniques have been devised in order to find a good approximation to the true solution, including Finite Element Methods and Boundary Element Methods. However, high wave frequencies can be difficult to approximate numerically, which can pose problems due to the often highly oscillatory nature of the solution. Thus it is advantageous to use a numerical method that approximates these high frequencies well, in addition to demonstrating fast convergence and low storage and computational costs.

1.2 Aims and Outline

We aim first of all to study and explain the theory that allows a problem over an infinite exterior domain to be reformulated into a boundary integral equation over a finite domain, and the problem of non-unique solutions that may arise from this process. We aim to consider methods that achieve a good approximate solution numerically even at high wave frequencies whilst minimising computational expense. We begin with some background of the direct scattering problem using the Helmholtz equation in Chapter 2, giving details of the general case in §2.1 and setting up a specific problem to solve in §2.4. We explain in §2.2 how it is possible to reformulate a problem of the entire domain into one involving just the boundary using Green's Representation Theorem. This will be beneficial numerically speaking as there is no need to restrict an infinite domain, however the very process does give rise to issues compromising the uniqueness of the solutions, as explained in §2.3. The use of a coupled formulation as originally proposed by Burton and Millar in [2] does overcome these issues of non-uniqueness, as explained in §2.3, at the cost of extra computational expense however.

In Chapter 3 we consider various Boundary Element Methods (BEM) that can be used to solve numerically our boundary integral equations. The use of the coupled formulation in numerical methods can be used to obtain any desired level of accuracy, but at a high computational expense. Standard schemes often fail for certain wavenumbers if not using the coupled formulation. Details for the programming of a collocation BEM and some numerical results demonstrating this failing are presented in §3.1.3 and §3.2. We then give details in Chapter 4 of a novel hybrid Galerkin BEM proposed by Langdon and Chandler-Wilde [1]. The method is specifically designed to find the unique exterior solution based upon careful study of its behaviour, avoiding spurious interior solutions. It is hoped this will remove the need to use the coupled formulation in some cases where only a set level of accu-

racy is required, thus avoiding extra computing expense. We then conclude our findings and present some possible research ideas for further expansion around the subject in Chapter 5.

Chapter 2

Background

2.1 Scattering Problems

Direct scattering problems are those which aim to find the scattered field produced by the interaction of a known incident wave with an object, based upon knowledge of the differential equation governing the wave motion. The inverse scattering problem is that of trying to determine the nature of the object or domain of definition, based upon the behaviour of the scattered wave. The total wave u is the sum of the known incident wave u^i and the scattered wave u^s, which is produced by the reflection and diffraction of u^i from a boundary Γ, as per Figure 2.1. Dirichlet boundary conditions $u = 0$ on the boundary Γ are referred to as being sound-soft in the case of acoustic scattering, whereas Neumann boundary conditions $\partial u/\partial n = 0$ on Γ are referred to as being sound-hard, as there is no flow across the boundary.

For acoustic waves, the velocity potential $U = U(x, t)$ satisfies the wave equation

$$\frac{1}{c^2}U_{tt} = \nabla^2 U = \frac{\partial^2 U}{\partial x^2} + \frac{\partial^2 U}{\partial y^2}, \tag{2.1}$$

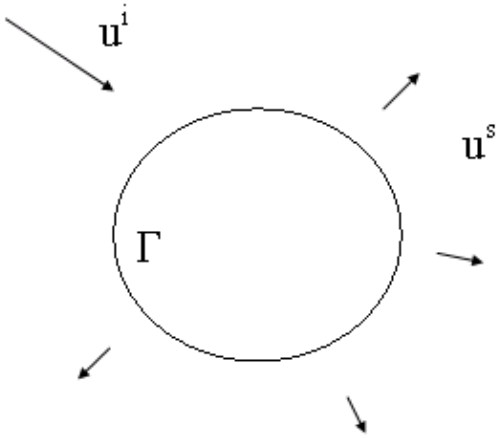

Figure 2.1: Total wave field comprising incident wave u^i and scattered wave u^s

(in two dimensions) and is time harmonic if

$$U = \Re\{e^{-i\omega t}u(\mathbf{x})\}.$$

The wave number $k = \omega/c$ depends upon the wave frequency $\omega > 0$ and the speed of sound c. It follows that

$$\frac{\partial^2 U}{\partial t^2} = -\omega^2 e^{-i\omega t}u(\mathbf{x}) = -k^2 c^2 e^{-i\omega t}u(\mathbf{x}),$$

and substituting this into (2.1) we have

$$-k^2 e^{-i\omega t}u(\mathbf{x}) = e^{-i\omega t}\nabla^2 u(\mathbf{x}).$$

By rearranging we are left with the Helmholtz equation

$$\nabla^2 u + k^2 u = 0 \tag{2.2}$$

which is satisfied by u^i, u^s and $u = u^i + u^s$. The Helmholtz equation is elliptic, and the use of Green's functions is particularly appropriate for solving this type of partial differential equation [3]. The fundamental solution of the Helmholtz equation is the Green's function

$$\Phi(\mathbf{x}, \mathbf{y}) = \frac{\mathrm{i}}{4} H_0^1(k|\mathbf{x} - \mathbf{y}|) \tag{2.3}$$

for the 2D case, or

$$\Phi(\mathbf{x}, \mathbf{y}) = \frac{e^{\mathrm{i}k|\mathbf{x}-\mathbf{y}|}}{4\pi|\mathbf{x} - \mathbf{y}|} \tag{2.4}$$

for the 3D case, where H_0^1 denotes the Hankel function of the first kind of order zero. In both the 2D and 3D case, $\Phi(\mathbf{x}, \mathbf{y})$ is singular at $\mathbf{x} = \mathbf{y}$, and $|\Phi(\mathbf{x}, \mathbf{y})| \to \infty$ as $\mathbf{x} \to \mathbf{y}$, as explained in [4] and [7]. The Hankel function is also known as a Bessel function of the third kind, so called as it comprises a complex linear combination of Bessel's functions of the first kind $J_\nu(x)$, and second kind $Y_\nu(x)$, resulting in

$$H_\nu^1(x) = J_\nu(x) + iY_\nu(x).$$

The first and second kind Bessel functions are so called as they are linearly independent solutions of Bessel's equation

$$x^2y'' + xy' + (x^2 - \nu^2)y = 0.$$

2.2 Boundary Integral Formulation

The main advantage of using integral equation methods in the solution of boundary value problems is that they allow the problem to be reduced from one involving the whole domain of interest to one involving just the boundary, reducing the dimension of the problem by one. This is especially benificial for exterior problems where the region of interest is infinite, such as the exterior

problem as we are considering, as it means that when solving numerically there is no need to restrict the domain.

From [2], the solution of the Helmholtz equation (2.2), when combined with the Sommerfield radiation condition (which will be defined in detail later), satisfies a form of Green's Representation Theorem

$$u_i(\mathbf{x}) + \int_\Gamma u(\mathbf{y}) \frac{\partial}{\partial n_y} \Phi(\mathbf{x}, \mathbf{y}) - \Phi(\mathbf{x}, \mathbf{y}) \frac{\partial}{\partial n} u(\mathbf{y}) dS_y = \begin{cases} u(\mathbf{x}) & (\mathbf{x} \in E), \\ \frac{1}{2} u(\mathbf{x}) & (\mathbf{x} \in \Gamma), \\ 0 & (\mathbf{x} \in \Omega), \end{cases} \tag{2.5}$$

where E is the exterior domain, Ω is the interior domain surrounded by boundary Γ, and $\frac{\partial}{\partial n}$ denotes the outward normal derivative.

If we first consider the top line of (2.5), and apply a Dirichlet boundary condition $u = 0$ (as we shall be considering later), by taking the normal derivative with respect to $\mathbf{x}$ and letting $\mathbf{x}$ tend to the boundary, we have

$$\frac{1}{2} \frac{\partial u}{\partial n}(\mathbf{x}) = \frac{\partial u^i(\mathbf{x})}{\partial n} - \int_\Gamma \frac{\partial \Phi(\mathbf{x}, \mathbf{y})}{\partial n_x} \frac{\partial u(\mathbf{y})}{\partial n} \mathrm{d}S_y \quad \mathbf{x} \in \Gamma \tag{2.6}$$

where the $\frac{1}{2} \frac{\partial u}{\partial n}$ term comes from a jump condition as $\mathbf{x}$ tends to Γ [5]. Alternatively from (2.5), again applying a Dirichlet boundary condition $u = 0$ we have

$$u^i(\mathbf{x}) - \int_\Gamma \Phi(\mathbf{x}, \mathbf{y}) \frac{\partial u(\mathbf{y})}{\partial n} \mathrm{d}S_y = 0, \quad \mathbf{x} \in \Gamma. \tag{2.7}$$

Equations (2.6) and (2.7) are each boundary integral equations that we could use to solve for $\frac{\partial u}{\partial n}$. Both are inhomogeneous Fredholm equations: (2.6) is of the second kind with kernel $\frac{\partial}{\partial n_x} \Phi(\mathbf{x}, \mathbf{y})$, whereas (2.7) is of the first kind with kernel $\Phi(\mathbf{x}, \mathbf{y})$. Once $\frac{\partial u}{\partial n}$ has been computed from (2.6) or (2.7), the first equation in (2.5) then gives a formula for $u(\mathbf{x})$ at any point $\mathbf{x} \in E$.

2.3 Uniqueness of Solutions

As we have seen in §2.2, it is possible to reformulate a problem over an entire domain into one involving just the boundary, using Green's Representation Theorem. Unfortunately, as per [2], due to the reformulation of the problem as a boundary integral equation, there may arise non-unique solutions that were not inherent to the original problem. Although the boundary values of $u(\mathbf{x})$ satisfy the integral equation (2.7), the solution of (2.7) may not be unique. There exist an infinite set of values of k for which the equation has a multiplicity of solutions, which coincide with the 'resonant' wavenumbers for a related interior problem.

To explain this we start with two well known theorems of Fredholm integral equations. The first is a fundamental theorem of integral equations, as explained in [3].

Theorem 2.1 *The Fredholm Alternative*

If the homogeneous equation

$$\psi + \lambda \int_\Gamma K(\mathbf{x}, \mathbf{y})\psi(\mathbf{y}) \mathrm{d}S_y = 0, \tag{2.8}$$

for boundary Γ and scalar λ, only possesses the trivial solution $\psi = 0$, then the inhomogeneous equation

$$\psi + \lambda \int_\Gamma K(\mathbf{x}, \mathbf{y})\psi(\mathbf{y}) \mathrm{d}S_y = f \tag{2.9}$$

will have a unique solution, for all square integrable functions f and kernels $K(\mathbf{x}, \mathbf{y})$.

Proof. Suppose ψ_1 and ψ_2 are two linearly independant solutions of (2.9), so we have

$$\psi_1 + \lambda \int_\Gamma K(\mathbf{x}, \mathbf{y})\psi_1(\mathbf{y}) \mathrm{d}S_y = f, \tag{2.10}$$

and

$$\psi_2 + \lambda \int_\Gamma K(\mathbf{x}, \mathbf{y})\psi_2(\mathbf{y})\mathrm{d}S_y = f. \tag{2.11}$$

Then taking (2.10) from (2.11) results in

$$(\psi_2 - \psi_1) + \lambda \int_\Gamma K(\mathbf{x}, \mathbf{y})(\psi_2(\mathbf{y}) - \psi_1(\mathbf{y}))\mathrm{d}S_y = 0, \tag{2.12}$$

an equation of the form (2.8) for $\psi_2 - \psi_1$. Thus, if there is only the trivial solution to (2.8), we conclude that $\psi_2 = \psi_1$: the solution to (2.9) is unique. ■

As quoted by Burton and Millar in [2], our second theorem:

Theorem 2.2 *If the homogeneous equation*

$$\frac{1}{2}\phi + \int_\Gamma \phi(\mathbf{y})\frac{\partial}{\partial n_x}\Phi(\mathbf{x}, \mathbf{y})\mathrm{d}S_y = 0 \tag{2.13}$$

with boundary Γ *and* $\Phi(\mathbf{x}, \mathbf{y})$ *given by (2.3), has a non trivial solution* ϕ*, then the transposed equation*

$$\frac{1}{2}\psi + \int_\Gamma \psi(\mathbf{y})\frac{\partial}{\partial n_y}\Phi(\mathbf{x}, \mathbf{y})\mathrm{d}S_y = 0 \tag{2.14}$$

will also possess a non-trivial solution ψ*, and conversely.*

The implication of Theorems 2.1 and 2.2 is that (2.6), which has a solution $\frac{\partial u}{\partial n}$ where $u(\mathbf{x})$ solves (2.2), and can be rearranged into

$$\frac{1}{2}\frac{\partial u}{\partial n}(\mathbf{x}) + \int_\Gamma \frac{\partial \Phi(\mathbf{x}, \mathbf{y})}{\partial n_x}\frac{\partial u(\mathbf{y})}{\partial n}\mathrm{d}S_y = \frac{\partial u^i(\mathbf{x})}{\partial n} \quad \mathbf{x} \in \Re^2 \backslash \Omega, \tag{2.15}$$

an inhomogeneous equation in the form (2.9), will have non unique solutions if the homogeneous equations in the form of (2.13) and (2.14) have non trivial solutions for some ϕ and ψ.

Consider now the interior problem

$$\nabla^2 v + k^2 v = 0 \quad \text{in } \Omega \tag{2.16}$$

and

$$\partial v/\partial n = 0 \quad \text{on } \Gamma. \tag{2.17}$$

This in general only has the solution $v \equiv 0$ unless k is one of an infinite set K_1 of discrete resonant eigenvalues for which there exists a non-trivial solution. Similar to (2.5), we have the Green's formulation for v solving (2.16):

$$\frac{1}{2}v(\mathbf{x}) + \int_\Gamma v(\mathbf{y})\frac{\partial}{\partial n_y}\Phi(\mathbf{x},\mathbf{y}) - \Phi(\mathbf{x},\mathbf{y})\frac{\partial}{\partial n}v(\mathbf{y})\mathrm{d}S_y = 0 \quad (\mathbf{x} \in \Gamma). \tag{2.18}$$

Applying $\partial v/\partial n = 0$, we obtain

$$\frac{1}{2}v(\mathbf{x}) + \int_\Gamma v(\mathbf{y})\frac{\partial}{\partial n_y}\Phi(\mathbf{x},\mathbf{y})\mathrm{d}S_y = 0 \quad (\mathbf{x} \in \Gamma)$$

which is an equation to solve for v in the form of (2.14). If $k \in K_1$, there is a non trivial solution v, and hence the solution to (2.15) will be non unique. That is to say, there are other solutions to (2.15) besides $\frac{\partial u}{\partial n}$ where u solves (2.2).

As explained in [2], (2.7) will also have the same defect: there are a multiplicity of solutions whenever $k \in K_2$, the set of eigenvalues for the interior Dirichlet problem. It is possible when trying to solve (2.6) or (2.7) for $\frac{\partial u}{\partial n}$ that a numerical scheme might pick up an eigenfunction of the related interior problem. Nevertheless, the two equations (2.6) and (2.7) always have only one solution in common.

As suggested by [2] and [1], to avoid obtaining an over-determined system of equations, we instead add a multiple $i\eta$ of (2.7) to (2.6), where $\eta \in \Re\backslash 0$,

resulting in

$$\frac{1}{2}\frac{\partial u(\mathbf{x})}{\partial n}+\int_\Gamma\left[\frac{\partial\Phi(\mathbf{x},\mathbf{y})}{\partial n_x}+i\eta\Phi(\mathbf{x},\mathbf{y})\right]\frac{\partial u(\mathbf{y})}{\partial n}\mathrm{d}S_y=\frac{\partial u^i(\mathbf{x})}{\partial n}+i\eta u^i(\mathbf{x}),\quad \mathbf{x}\in\Gamma. \tag{2.19}$$

This can be written as

$$(I+\kappa)\frac{\partial u}{\partial n}=f\quad \mathbf{x}\text{ on }\Gamma \tag{2.20}$$

where

$$\kappa v(\mathbf{x})=2\int_\Gamma\left[\frac{\partial\Phi(\mathbf{x},\mathbf{y})}{\partial n_x}+i\eta\Phi(\mathbf{x},\mathbf{y})\right]v(\mathbf{y})\mathrm{d}S_y \tag{2.21}$$

and

$$f(\mathbf{x})=2\left[\frac{\partial u^i(\mathbf{x})}{\partial n}+i\eta u^i(\mathbf{x})\right]. \tag{2.22}$$

By choosing $\eta\neq 0$ in (2.19), we can solve to find a unique $\partial u/\partial n$. Generally, solving either (2.19) or, by taking $\eta=0$, (2.6) will result in the same solution. However if k is an eigenvalue of the related interior Neumann problem (2.16)-(2.17), (2.6) will have a multiplicity of solutions. To solve (2.19) numerically is more expensive computationally than to solve (2.6) as it requires the evaluation of more Hankel functions, and this is expensive computationally.

The choice of coupling parameter η has received much attention in the literature of recent years. As explained in [1], in this case $\eta=k$ is the optimal choice for finding the exterior solution and ensuring the system is well conditioned. Unfortunately, this choice could potentially double the computing time compared to choosing $\eta=0$. As can be seen in Table 2.1, the computation time in Matlab for the evaluation of Hankel functions grows at a rate similar to that of the increase in the number to be evaluated. It is therefore of interest to determine whether it is necessary to use (2.19) or whether numerical schemes for (2.6) do in fact converge to the required solution of the exterior problem (2.2).

Table 2.1: Evalution Time of Hankel Functions

Number of Hankel functions	Time (seconds)
1	3.72×10^{-4}
10	8.72×10^{-4}
100	1.041×10^{-3}
1000	2.5799×10^{-2}

2.4 A Specific Problem

We will consider in this project the scattering of acoustic waves by a convex polygon in two dimensions, solving the Helmholtz equation

$$\nabla^2 u + k^2 u = 0 \quad \text{in } E. \tag{2.23}$$

We will consider the sound-soft case of Dirichlet boundary conditions

$$u(\mathbf{x}) = 0 \quad \text{on } \Gamma, \tag{2.24}$$

and so solve for the unknown $\frac{\partial u}{\partial n}$ by reformulating (2.23) as a boundary integral equation given by (2.20). Our bounded domain Ω is chosen to be square, $0 \leq x \leq L$, $0 \leq y \leq L$, which causes the reflection and defraction of the incident wave u^i, producing the scattered wave u^s, as per Figure 2.2.

The wave number $k = 2\pi/\lambda$, where λ is the wavelength of the incident wave, so it is proportional to the frequency of the incident wave. We consider the case of an incident plane wave given by

$$u^i = e^{\mathrm{i}k\mathbf{x}\cdot\mathbf{d}} = e^{\mathrm{i}k(x_1,x_2)\cdot(\sin\theta,-\cos\theta)} \tag{2.25}$$

where $\mathbf{x} = (x_1, x_2)$, the direction of propagation $\mathbf{d} := (\sin\theta, -\cos\theta)$, and $\theta \in [0, 2\pi)$ is the angle of incidence, as measured anticlockwise from the

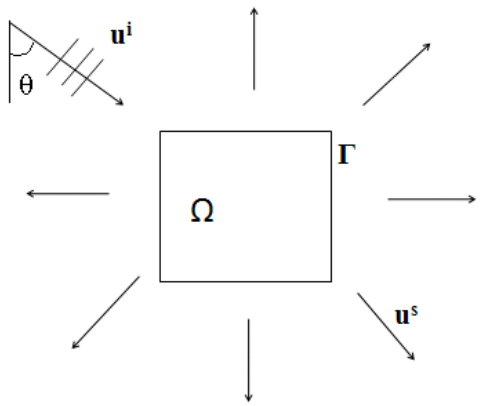

Figure 2.2: Reflection of u^i on a square domain.

downward vertical. The scattered field must also satisfy the Sommerfeld radiation condition

$$\lim_{r\to\infty} r^{1/2}\left(\frac{\partial u^s}{\partial r} - \mathrm{i}ku^s\right) = 0 \tag{2.26}$$

uniformly in $\mathbf{r}$, where $\mathbf{r} = \mathbf{x}/|\mathbf{x}|$ is a unit vector in the direction of $\mathbf{x}$, and $r = |\mathbf{x}|$. This condition ensures u^s is an outgoing wave, so the scattered field is not reflected back from infinity.

2.5 Eigenvalues of the Interior Neumann Problem

In order to investigate for which values of k the equation (2.20) with $\eta = 0$ has a non-unique solution, we must consider the related interior problem, as explained in §2.3. We wish to find u that satisfies the Helmholtz equation

$$\nabla^2 u + k^2 u = 0 \quad \text{in } \Omega, \tag{2.27}$$

on the interior of the square domain $0 \leq x \leq L$, $0 \leq y \leq L$, with Neumann boundary conditions

$$\frac{\partial u}{\partial n} = 0 \quad \text{on } \Gamma \tag{2.28}$$

on the boundary. We wish to find the eigenvalues k for which there are non trivial solutions, and the corresponding eigenfunctions. These will be the values of k for which (2.6) and (2.7) will not have a unique solution. These solutions are those which we expect our Boundary Element Methods to pick up when we use values k that are eigenvalues when trying to find the solution to the exterior Dirichlet problem, that is (2.23) and (2.24) in $\Re^2 \backslash \Omega$.

Using standard separation of variables techniques, we set $u(x, y) = X(x)Y(y)$. From the Helmholtz equation we obtain

$$X''Y + XY'' + k^2 XY = 0$$

which rearranges to

$$\frac{X''}{X} + k^2 = -\frac{Y''}{Y} = \alpha$$

where α is our separation constant. Rearranging, we obtain

$$X'' + (k^2 - \alpha)X = 0 \qquad (0 < x < L) \tag{2.29}$$

$$Y'' + \alpha Y = 0 \qquad (0 < y < L). \tag{2.30}$$

Note that, by the symmetry of the problem we could equally solve

$$Y'' + (k^2 - \alpha)Y = 0 \qquad (0 < y < L),$$

$$X'' + \alpha X = 0 \qquad (0 < x < L).$$

Our Neumann boundary condition (2.28) results in $X'(0) = X'(L) = 0$ and $Y'(0) = Y'(L) = 0$, and we shall use (2.29) and (2.30)to solve for our

solution $u(x, y)$.

First considering the case $\alpha = 0$, we obtain

$$Y = Ay + B,$$

and

$$X = C\cos(kx) + D\sin(kx),$$

where A, B, C, D are constants. The boundary conditions result in $A = 0$, $D = 0$ and $k = n\pi/L$ $(n \in N)$ for non trivial solutions. This therefore results in

$$u_n(x, y) = C_n \cos(\frac{n\pi}{L}x). \tag{2.31}$$

For the case of negative α, say $\alpha = -\gamma^2 < 0$ we have

$$Y = A\cosh(\gamma y) + B\sinh(\gamma y),$$

which results only in the trivial solution $Y = 0$ when boundary conditions are applied.

For positive α, we set $\alpha = \beta^2 > 0$. For

$$Y = A\cos(\beta y) + B\sin(\beta y),$$

the boundary conditions imply $B = 0$ and $\beta = \frac{m\pi}{L}$ $(m \in N)$ for a non-trivial solution. For

$$X'' + (k^2 - \frac{m^2\pi^2}{L^2})X = 0$$

we need to consider the different sizes of k. First considering the case $k = \frac{m\pi}{L}$, we obtain $X = D$, a constant, so that

$$u_m(x, y) = A_m \cos(\frac{m\pi}{L}y). \tag{2.32}$$

The case $k < \frac{m\pi}{L}$ when combined with boundary conditions results only in the trivial solution. For $k > \frac{m\pi}{L}$, we obtain

$$X = C\cos(\sqrt{k^2 - \beta^2}x) + D\sin(\sqrt{k^2 - \beta^2}x).$$

Combined with the boundary conditions it follows that $D = 0$ and

$$k = \frac{\pi}{L}\sqrt{n^2 + m^2} \quad (n, m \in N), \tag{2.33}$$

to ensure non trivial solutions. The eigenfunctions are then given by

$$u_{m,n}(x, y) = A_m C_n \cos(\frac{n\pi}{L}x)\cos(\frac{m\pi}{L}y). \tag{2.34}$$

Thus, the general solution for our problem, (2.27) and (2.28), is given by the sum of our (2.31), (2.32), and (2.34) solutions:

$$u(x, y) = \sum_{n=0}^{\infty}\sum_{m=0}^{\infty} A_{m,n}\cos(\frac{n\pi}{L}x)\cos(\frac{m\pi}{L}y), \tag{2.35}$$

where $A_{m,n}$ is a constant that depends upon m and n.

Chapter 3

Solving the Boundary Integral Equation

3.1 Boundary Element Methods

Boundary Element Methods (BEM) are those where we solve the boundary integral equation rather than solving the boundary value problem directly. The original boundary value problem is reformulated from one involving the whole space into one involving just the boundary using integral equation formulations, typically using Green's identities, as seen in Chapter 2. This reduces the dimension size of the problem, so in three dimensions the problem is evaluated over a surface, and a two dimensional problem is reduced to solving a one dimensional problem over the boundary. To do this the boundary is discretised into elements over which a finite set of basis functions are used to approximate the space. These basis functions are usually low degree polynomials chosen to satisfy appropriate continuity properties at inter-element boundaries. Approximate solutions to the resulting discrete problem are then obtained numerically by using suitable approximate integration techniques over the boundary. The integral equation can then be

used to calculate the solution at points in the original solution domain.

Two common boundary element methods are the collocation and Galerkin methods, as detailed in [6]. These methods use approximations for the solution u of the form

$$u(x) = \sum_{j=1}^{M} u_j \chi_j(x) \tag{3.1}$$

where $\chi_1, ..., \chi_M$ is the set of basis functions. The resultant matrix systems in these BEMs are full, meaning they require higher storage and computational time to solve than those which arise in typical Finite Difference (FD) and Finite Element Methods (FEM). BEM leads to small, dense systems, whilst FD and FEM lead to large, sparse systems.

3.1.1 Collocation Method

The boundary is split into a chosen set of "collocation points" $s_1, ..., s_M$. The collocation method finds the solution u such that

$$Lu(s_k) = f(s_k), \quad k = 1, ..., M \tag{3.2}$$

where L is the linear operator mapping real or complex functions on the boundary Γ to other functions on Γ, and f is some right hand-side. This gives M equations for one unknown, however writing u in the form (3.1) results in

$$\sum_{j=1}^{M} Lu_j \chi_j(s_k) = f(s_k), \quad k = 1, ..., M \tag{3.3}$$

giving M equations for the M unknowns. This results in a full matrix system, with each matrix element requiring the evaluation of single integrals in the two-dimensional case, double integrals in the three-dimensional case.

For the 2D case with boundary $\Gamma : x \in [a, b]$, to solve the problem

$$u(x) + \int_a^b K(x, y)u(y)\mathrm{d}y = f(x) \tag{3.4}$$

using a simple collocation method we write u as in (3.1), and choose the piecewise constant basis functions

$$\chi_j(x) = \begin{cases} 1 & x \in [x_{j-1}, x_j] \\ 0 & \text{elsewhere} \end{cases}, \tag{3.5}$$

where $x_j = a + \frac{j}{M}(b - a)$ for the points on the boundary

$$a = x_0 < x_1 < ... < x_M = b.$$

Substituting this into (3.4) it follows that

$$\sum_{j=1}^{M} u_j[\chi_j(x) + \int_a^b K(x, y)\chi_j(y)\mathrm{d}y] = f(x). \tag{3.6}$$

We choose the collocation points s_m to be the mid points of each interval $[x_{j-1}, x_j]$ and forcing (3.6) to hold at each of these gives the M equations. The resultant matrix system is

$$[\chi + K]\,\mathbf{u} = \mathbf{f} \tag{3.7}$$

where

$$\mathbf{u} = \begin{pmatrix} u_1 \\ u_2 \\ \vdots \\ u_M \end{pmatrix} \tag{3.8}$$

is a vector of unknowns,

$$\chi = \begin{pmatrix} \chi_1(s_1) & \chi_2(s_1) & \dots & \\ \chi_1(s_2) & \ddots & & \\ \vdots & & \ddots & \vdots \\ & & \dots & \chi_M(s_M) \end{pmatrix} = I, \tag{3.9}$$

the identity matrix,

$$\mathrm{K}= \begin{pmatrix} \int_a^b K(s_1,y)\chi_1(y)\mathrm{d}y & \int_a^b K(s_1,y)\chi_2(y)\mathrm{d}y & \dots & \\ \int_a^b K(s_2,y)\chi_1(y)\mathrm{d}y & \ddots & & \\ \vdots & & \ddots & \vdots \\ & & \dots & \int_a^b K(s_M,y)\chi_M(y)\mathrm{d}y \end{pmatrix}$$

$$= \begin{pmatrix} \int_{x_0}^{x_1} K(s_1,y)dy & \int_{x_1}^{x_2} K(s_1,y)dy & \dots & \\ \int_{x_0}^{x_1} K(s_2,y)dy & \ddots & & \\ \vdots & & \ddots & \vdots \\ & & \dots & \int_{x_{M-1}}^{x_M} K(s_M,y)dy \end{pmatrix}, \tag{3.10}$$

and

$$\mathbf{f} = \begin{pmatrix} f(s_1) \\ \vdots \\ \\ f(s_M) \end{pmatrix}. \tag{3.11}$$

For our wave scattering problem (2.20), the kernel is given by

$$K(\mathbf{x},\mathbf{y}) = 2i\eta H_0^1(k|\mathbf{x}-\mathbf{y}|) + 2\frac{\partial}{\partial n(\mathbf{x})} H_0^1(k|\mathbf{x}-\mathbf{y}|). \tag{3.12}$$

3.1.2 Galerkin Method

Galerkin methods solve the problem $Lu = f$ for u by finding a weak solution such that

$$(Lu, \chi_j) = (f, \chi_j) \quad \text{for all } \chi_j, \tag{3.13}$$

where

$$(v, w) := \int_\Gamma v\overline{w} d\Gamma$$

denotes the inner product, and $\overline{w}$ is the complex conjugate of w. If the function is real then $\overline{w} = w$. Writing u as in (3.1) the equations to be solved are

$$\sum_{j=1}^{M} (L\chi_j, \chi_k) u_j = (f, \chi_k), \quad k = 1, ..., M. \tag{3.14}$$

This means that each matrix element $(L\chi_j, \chi_k)$ is a two dimensional integral, one integral for the integral operator L, the other for the inner product.

3.1.3 The Program

Due to the extra computational expense caused by the double integrals involved in Galerkin methods, we will aim to solve (2.20) using a collocation BEM for the problem defined in §2.4. In terms of programing (3.7) numerically in a code in Matlab, consideration had to be taken as to which side of the square region the mid points s_k were on when computing the normal derivatives. We split the boundary Γ into the four separate sides of length $L = 2\pi$: Γ_1 denoting $0 \leq x \leq 2\pi$, $y = 0$; Γ_2 denoting $x = 2\pi$, $0 \leq y \leq 2\pi$; Γ_3 denoting $0 \leq x \leq 2\pi$, $y = 2\pi$; and Γ_4 denoting $x = 0$, $0 \leq y \leq 2\pi$. The outward normal vectors $\mathbf{n} = (n_1, n_2)^T$ for these four sides are $(0, -1)^T$, $(1, 0)^T$, $(0, 1)^T$, and $(-1, 0)^T$ respectively, as shown in Figure 3.1, where $\mathbf{n_i}$ denotes the outward normal on Γ_i.

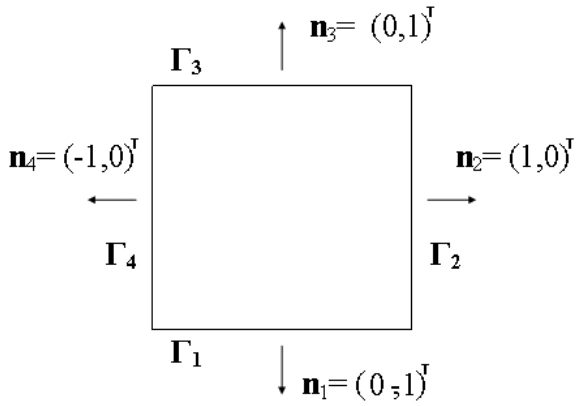

Figure 3.1: Outward normal derivative vectors

For the normal derivative of the incident wave we have,

$$\frac{\partial u^i}{\partial n(\mathbf{x})} = \bigtriangledown u^i \cdot \mathbf{n} = \begin{pmatrix} \frac{\partial u^i}{\partial x_1} \\ \frac{\partial u^i}{\partial x_2} \end{pmatrix} \cdot \begin{pmatrix} n_1 \\ n_2 \end{pmatrix} \tag{3.15}$$

where $\mathbf{x} = (x_1, x_2)^T$, so that on Γ_1

$$\frac{\partial u^i}{\partial n} = -\frac{\partial u^i}{\partial x_2} = ik\cos(\theta)e^{ik(x_1\sin(\theta)-x_2\cos(\theta))},$$

on Γ_2

$$\frac{\partial u^i}{\partial n} = \frac{\partial u^i}{\partial x_1} = ik\sin(\theta)e^{ik(x_1\sin(\theta)-x_2\cos(\theta))},$$

on Γ_3

$$\frac{\partial u^i}{\partial n} = \frac{\partial u^i}{\partial x_2} = -ik\cos(\theta)e^{ik(x_1\sin(\theta)-x_2\cos(\theta))},$$

and on Γ_4

$$\frac{\partial u^i}{\partial n} = -\frac{\partial u^i}{\partial x_1} = -ik\sin(\theta)e^{ik(x_1\sin(\theta)-x_2\cos(\theta))}.$$

Similarly, for the normal dervivative of the fundamental solution

$$\frac{\partial\Phi(\mathbf{x},\mathbf{y})}{\partial n(\mathbf{x})} = \bigtriangledown\Phi(\mathbf{x},\mathbf{y})\cdot\mathbf{n} = \begin{pmatrix} \frac{\partial\Phi(\mathbf{x},\mathbf{y})}{\partial x_1} \\ \frac{\partial\Phi(\mathbf{x},\mathbf{y})}{\partial x_2} \end{pmatrix}\cdot\begin{pmatrix} n_1 \\ n_2 \end{pmatrix}, \tag{3.16}$$

where $\mathbf{y} = (y_1, y_2)^T$. From [4],

$$\frac{\mathrm{d}}{\mathrm{d}z}H_0^1(z) = -H_1^1(z),$$

so that on Γ_1

$$\frac{\partial\Phi}{\partial\mathbf{n}} = -\frac{\partial\Phi}{\partial x_2} = \frac{k(x_2-y_2)}{|\mathbf{x}-\mathbf{y}|}H_1^1(k|\mathbf{x}-\mathbf{y}|),$$

on Γ_2

$$\frac{\partial\Phi}{\partial\mathbf{n}} = \frac{\partial\Phi}{\partial x_1} = -\frac{k(x_1-y_1)}{|\mathbf{x}-\mathbf{y}|}H_1^1(k|\mathbf{x}-\mathbf{y}|),$$

on Γ_3

$$\frac{\partial\Phi}{\partial n} = \frac{\partial\Phi}{\partial x_2} = -\frac{k(x_2-y_2)}{|\mathbf{x}-\mathbf{y}|}H_1^1(k|\mathbf{x}-\mathbf{y}|),$$

and on Γ_4

$$\frac{\partial\Phi}{\partial\mathbf{n}} = -\frac{\partial\Phi}{\partial x_1} = \frac{k(x_1-y_1)}{|\mathbf{x}-\mathbf{y}|}H_1^1(k|\mathbf{x}-\mathbf{y}|).$$

3.2 Numerical Results

The standard BEM program was run for various values of k, chosen so as to compare the effectiveness of the method for those k which are eigenvalues of the interior problem, as given by (2.33), and those which are not. Recalling §2.3, we might expect the BEM to work well when k is not an eigenvalue, and to perform poorly when k is an eigenvalue, as in that case the BIE does not have a unique solution. When $\eta = k$ we expect the method to work well in all cases. Each side of the square was split into N collocation points, for $N = 2, 4, 8, 16, 32, 64, 128$. The program was used to test the importance

of the coupling parameter η in finding the unique solution to the exterior problem, rather than the spurious solutions related to the interior problem. When computing the L^2 error $||exact - approximate||_2$ and the relative error $||exact - approximate||_2/||exact||_2$, the exact solution was taken to be that resultant from $\eta = k$, $N = 128$. We would in theory expect these errors to halve each time we double the number of degrees of freedom N. However, as k increases the wave frequency increases, so we would expect to require a higher number of discretisation points N for an good approximation to the true solution. Supposing

$$error(N) = CN^P$$

for a constant C, we have

$$\frac{error(2N)}{error(N)} = \frac{C2^P N^P}{CN^P} = 2^P,$$

so that the Estimated Order of Convergence (EOC) is given by

$$P = \log_2(\frac{error(2N)}{error(N)}).$$

We would expect $P = -1$ as we are using piecewise constants, that is we would expect the error to decrease at a rate proportional to the rate the discretisation step decreases.

For graphical output, the four sides of the square were mapped to the X-axis, so that Γ_1 is represented on $0 \leq x \leq 2\pi$, Γ_2 on $2\pi \leq x \leq 4\pi$ Γ_3 on $4\pi \leq x \leq 6\pi$, and Γ_4 on $6\pi \leq x \leq 8\pi$. The sides in shadow, Γ_1 and Γ_2, have solutions consisting of just the diffracted waves, and hence these are smaller in magnitude than those on the illuminated sides Γ_3 and Γ_4 which also include the reflected wave.

Table 3.1 shows how the error and relative L^2 error decrease at a similar

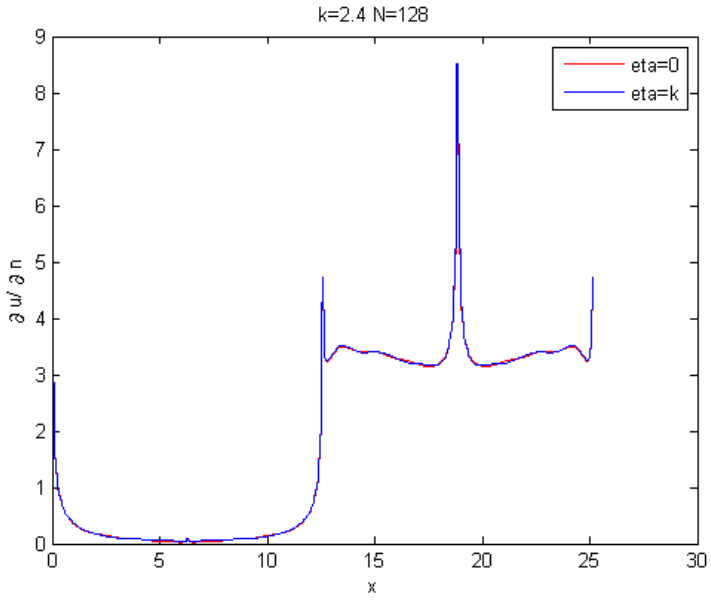

Figure 3.2: k not an eigenvalue

rate regardless of the value of η when k is not an eigenvalue. It is also clear that for a desired level of accuracy, as k increases we need to increase N.

For values of k that are not eigenvalues of the interior problem, the standard BEM easily converged to the correct solution even for $\eta = 0$, as shown in Figures 3.2 and 3.4. However, for values of k that are eigenvalues of the interior problem, the BEM clearly has problems finding the unique solution of the exterior problem when $\eta = 0$, as shown in Figure 3.3. As n and m increase, these eigenvalues become more frequent, and so as k increases it becomes more likely to find a spurious solution. Figures 3.6, 3.7, and 3.8 show how these eigenvalues start to have an influence even when k is not an eigenvalue: $k = 12.505$ is close to two eigenvalues $k = 12.5$ and $k = 12.51$, and its approximation with $\eta = 0$ is less accurate than for smaller k even though it is not actually an eigenvalue, although this may be due to the need for higher N to approximate the increased oscillation well.

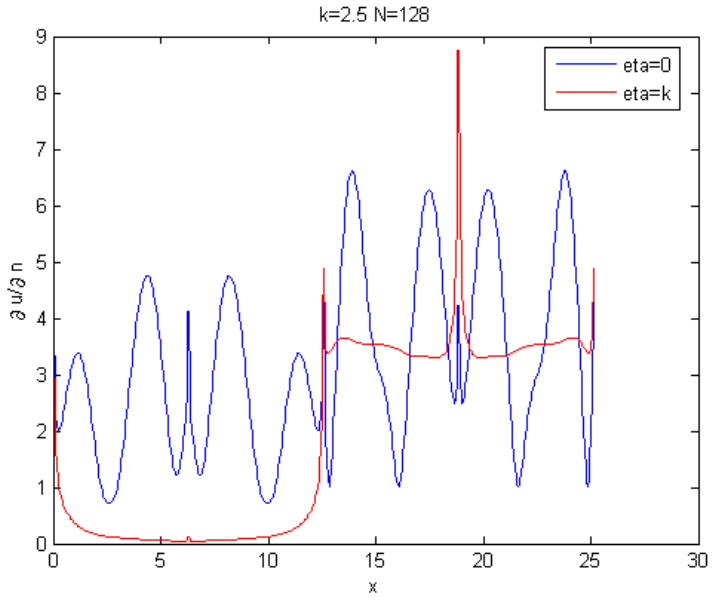

Figure 3.3: k an eigenvalue

Due to the spurious solutions that are being found when k is an eigenvalue, the error and relative L^2 errors fluctuate when $\eta = 0$, as shown in Table 3.2, and so don't converge even for high N, as shown in Figure 3.10. This is also evident in Figure 3.9; only at interior eigenvalues of k does the L^2 error increase. This graph only peaks for those values of k tested, if all values were tested we would expect the number of peaks to increase as $k \to \infty$, which would make this collocation BEM a poor numerical method for the solving of high frequency problems whilst minimising computational expense. Figure 3.5 shows the absolute error $|\text{exact} - \text{approx}|$ for k's that are not eigenvalues, the exact taken from the coupled formulation ($\eta = k$) and $N = 128$, the approximate using $\eta = 0$, which we would ideally like to use to minimise computational expense as there is least risk of spurious solutions in this case. It is clear that the error is largest near the corners of the square. We would expect the solution to be peaked here as the deffracted waves decay along the

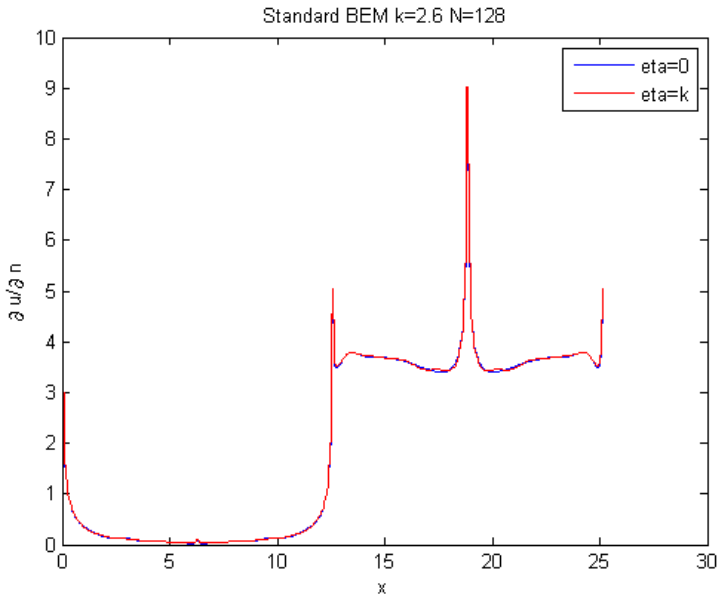

Figure 3.4: k not an eigenvalue

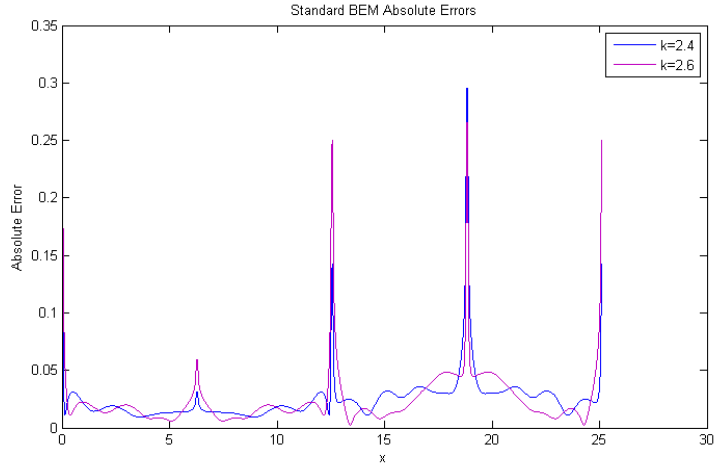

Figure 3.5: Absolute Errors when k is not an eigenvalue, N=128

square's sides. So perhaps in future work more consideration of this should be taken into account when discretising our boundary.

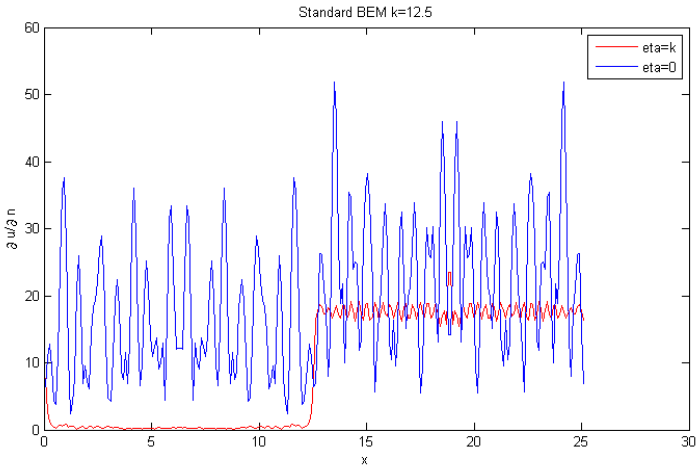

Figure 3.6: k an Eigen-value, N=128

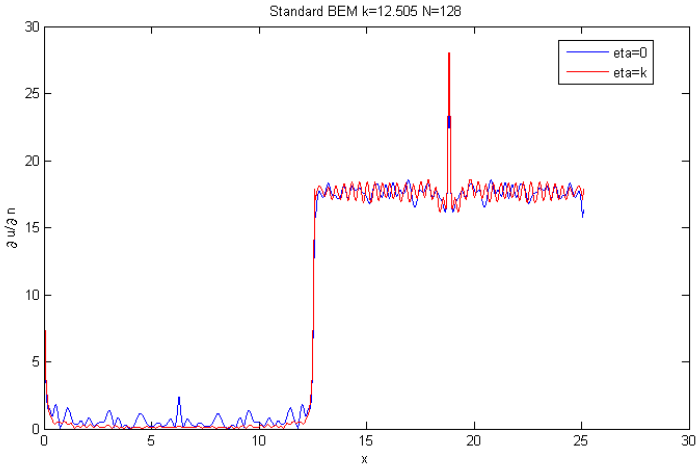

Figure 3.7: k not an Eigen-value

Table 3.1: Relative L2 errors for the case that k is not an eigenvalue.

		$\eta = 0$			$\eta = k$		
k	N	$\|\|\text{error}\|\|_2$	$\|\|\text{Relative error}\|\|_2$	EOC	$\|\|\text{error}\|\|_2$	$\|\|\text{Relative error}\|\|_2$	EOC
2.4	2	1.1361×10^{1}	6.0455×10^{-1}	0.8260	1.0592×10^{1}	5.6363×10^{-1}	0.0015
	4	2.01391×10^{1}	1.0717×10^{0}	-3.4840	1.0603×10^{1}	5.6420×10^{-1}	-2.2538
	8	1.7999×10^{0}	9.5779×10^{-2}	-1.0300	2.2231×10^{0}	1.1830×10^{-1}	-1.2550
	16	8.8147×10^{-1}	4.6905×10^{-2}	-0.5060	9.3149×10^{-1}	4.9567×10^{-2}	-0.6753
	32	6.2073×10^{-1}	3.3030×10^{-2}	-0.4564	5.8331×10^{-1}	3.1039×10^{-2}	-0.4400
	64	4.5239×10^{-1}	2.4073×10^{-2}	-2.8351	4.2997×10^{-1}	2.2880×10^{-2}	
	128	6.3398×10^{-2}	3.3735×10^{-3}				
2.6	2	3.9067×10^{1}	1.9528×10^{0}	-1.4319	7.2505×10^{0}	3.6242×10^{-1}	1.3057
	4	1.4480×10^{1}	7.2378×10^{-1}	-2.1251	1.7923×10^{1}	8.9591×10^{-1}	-2.3717
	8	3.3194×10^{0}	1.6592×10^{-1}	-0.6880	3.4631×10^{0}	1.7311×10^{-1}	-0.7468
	16	2.0604×10^{0}	1.0299×10^{-1}	-0.6422	2.0637×10^{0}	1.0316×10^{-1}	-0.6768
	32	1.3202×10^{0}	6.5989×10^{-2}	-0.7824	1.2910×10^{0}	6.4530×10^{-2}	-0.8032
	64	7.6751×10^{-1}	3.8365×10^{-2}	-2.6992	7.3983×10^{-1}	3.6981×10^{-2}	
	128	1.1818×10^{-1}	5.9074×10^{-3}		0		
4.9	2	1.2583×10^{1}	6.1878×10^{-1}	0.7670	2.9230×10^{1}	1.4374×10^{0}	-0.2541
	4	2.1413×10^{1}	1.0530×10^{0}	0.4739	2.4509×10^{1}	1.2053×10^{0}	-0.5005
	8	2.9740×10^{1}	1.4625×10^{0}	-3.0063	1.7325×10^{1}	8.5197×10^{-1}	-2.2244
	16	3.7012×10^{0}	1.8201×10^{-1}	-0.6303	3.7073×10^{0}	1.8231×10^{-1}	-0.6625
	32	2.3913×10^{0}	1.1759×10^{-1}	-0.7627	2.3422×10^{0}	1.1518×10^{-1}	-0.7464
	64	1.4093×10^{0}	6.9305×10^{-2}	-2.7672	1.3961×10^{0}	6.8657×10^{-2}	
	128	2.0700×10^{-1}	1.0180×10^{-2}				
12.505	2	4.1820×10^{1}	7.1743×10^{-1}	-1.6295	1.5814×10^{1}	2.7129×10^{-1}	1.4212
	4	1.3516×10^{1}	2.3187×10^{-1}	1.9743	4.2349×10^{1}	7.2652×10^{-1}	-0.8024
	8	5.3110×10^{1}	9.1113×10^{-1}	-0.9369	2.4282×10^{1}	4.1657×10^{-1}	0.6559
	16	2.7743×10^{1}	4.7593×10^{-1}	-0.3528	3.8258×10^{1}	6.5634×10^{-1}	-1.6708
	32	2.1724×10^{1}	3.7268×10^{-1}	-2.4218	1.2016×10^{1}	2.0614×10^{-1}	-1.3605
	64	4.0542×10^{0}	6.9551×10^{-2}	-0.4743	4.6797×10^{0}	8.0281×10^{-2}	
	128	2.9182×10^{0}	5.0063×10^{-2}				

Table 3.2: Relative L2 errors for the case that k is an eigenvalue.

		$\eta = 0$			$\eta = k$		
k	N	$\|\|\text{error}\|\|_2$	$\|\|\text{Relative error}\|\|_2$	EOC	$\|\|\text{error}\|\|_2$	$\|\|\text{Relative error}\|\|_2$	EOC
2.5	2	4.2036×10^{1}	2.1337×10^{0}	2.1866	9.2925×10^{0}	4.7169×10^{-1}	0.6261
	4	1.9136×10^{2}	9.7132×10^{0}	-4.3380	1.4342×10^{1}	7.2802×10^{-1}	-2.2385
	8	9.4617×10^{0}	4.8027×10^{-1}	0.2625	3.0392×10^{0}	1.5427×10^{-1}	-0.8842
	16	1.1349×10^{1}	5.7610×10^{-1}	0.1127	1.6466×10^{0}	8.3579×10^{-2}	-0.7975
	32	1.2272×10^{1}	6.2292×10^{-1}	0.0477	9.4733×10^{-1}	4.8086×10^{-2}	-0.8555
	64	1.2684×10^{1}	6.4385×10^{-1}	0.0196	5.2354×10^{-1}	2.6575×10^{-2}	
	128	1.2857×10^{1}	6.5265×10^{-1}				
5	2	1.0968×10^{1}	5.8400×10^{-1}	3.4245	2.1035×10^{1}	1.1200×10^{0}	0.1140
	4	1.1776×10^{2}	6.2702×10^{0}	1.4589	2.2764×10^{1}	1.2121×10^{0}	1.7471
	8	3.2373×10^{2}	1.7237×10^{1}	-3.3416	7.6415×10^{1}	4.0688×10^{0}	-4.8844
	16	3.1936×10^{1}	1.7004×10^{0}	0.6605	2.5873×10^{0}	1.3776×10^{-1}	-0.4640
	32	5.0477×10^{1}	2.6877×10^{0}	0.2371	1.8756×10^{0}	9.9870×10^{-2}	-0.5724
	64	5.9493×10^{1}	3.1677×10^{0}	0.0903	1.2614×10^{0}	6.7161×10^{-2}	
	128	6.3333×10^{1}	3.3722×10^{0}				
12.5	2	3.5982×10^{1}	6.1848×10^{-1}	-1.2645	1.6611×10^{1}	2.8553×10^{-1}	1.3987
	4	1.4977×10^{1}	2.5744×10^{-1}	1.8373	4.3798×10^{1}	7.5283×10^{-1}	-0.6760
	8	5.3522×10^{1}	9.1996×10^{-1}	-0.5991	2.7414×10^{1}	4.7121×10^{-1}	0.4003
	16	3.5334×10^{1}	6.0734×10^{-1}	0.3944	3.6182×10^{1}	6.2191×10^{-1}	-1.5862
	32	4.6442×10^{1}	7.9828×10^{-1}	0.8961	1.2050×10^{1}	2.0712×10^{-1}	-1.3584
	64	8.6429×10^{1}	1.4856×10^{0}	0.3941	4.6996×10^{0}	8.0780×10^{-2}	
	128	1.1358×10^{2}	1.9523×10^{0}				
12.51	2	4.1890×10^{1}	7.1720×10^{-1}	-1.7994	1.5079×10^{1}	2.5817×10^{-1}	1.4406
	4	1.2035×10^{1}	2.0605×10^{-1}	2.1400	4.0929×10^{1}	7.0074×10^{-1}	-0.9416
	8	5.3044×10^{1}	9.0817×10^{-1}	0.0040	2.1310×10^{1}	3.6485×10^{-1}	0.9251
	16	5.3189×10^{1}	9.1066×10^{-1}	-0.6646	4.0464×10^{1}	6.9278×10^{-1}	-1.7559
	32	3.3556×10^{1}	5.7451×10^{-1}	-1.5223	1.1981×10^{1}	2.0512×10^{-1}	-1.3627
	64	1.1682×10^{1}	2.0001×10^{-1}	-0.5549	4.6586×10^{0}	7.9760×10^{-2}	
	128	7.9519×10^{0}	1.3615×10^{-1}				

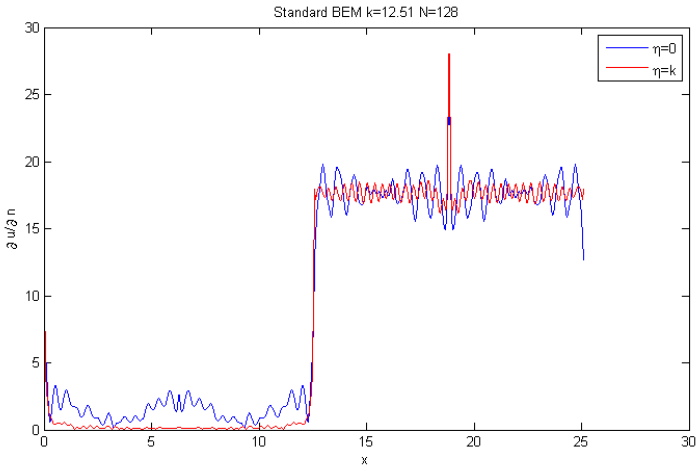

Figure 3.8: k an Eigen-value

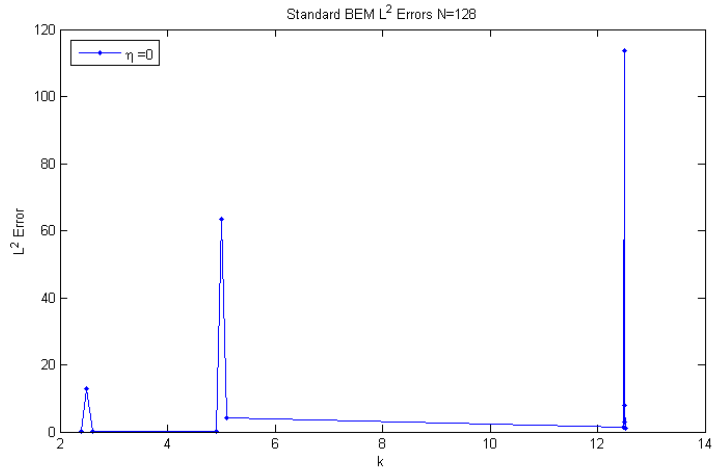

Figure 3.9: L^2 Errors against k

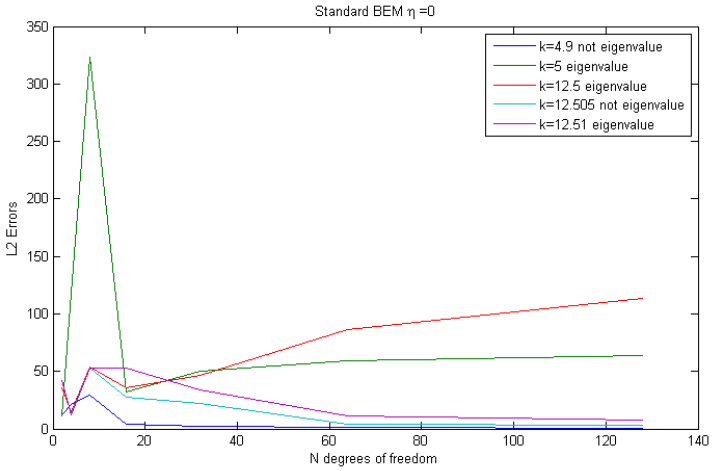

Figure 3.10: L^2 Errors against degrees of freedom, for various k

Chapter 4

Is the Coupled Layer Formulation Necessary?

The theory from [2], supported by results in Chapter 3, tells us that solving the Helmholtz equation (2.2) by reducing it to a boundary integral formulation (2.20) may produce spurious solutions which relate to an interior problem when the coupling parameter $\eta = 0$. However, there is still a unique solution to the exterior problem.

4.1 The Hybrid Boundary Element Method

In [1] Chandler-Wilde and Langdon carefully study the oscillatory behaviour of the solution to the exterior problem for scattering by a general convex polygon, and devise a hybrid Galerkin BEM specially designed to approximate the solution to the exterior problem rather than the interior solution, even when $\eta = 0$.

The scattering of waves by a square, as we are considering here is a simple case of scattering by a convex polygon, or an obstacle with corners.

The corners usually cause diffracted waves to illuminate the shadow side strongly, as they travel along the polygon's sides. As k increases, the leading order behavior on the illuminated sides Γ_3 and Γ_4 is made up of the incident plane wave and a known reflected wave, whereas these are zero on shadow sides Γ_1 and Γ_2. The method approximates the normal derivative solution by separating it into the leading order behaviour and a linear combination of the products of piecewise polynomials and plane waves travelling parallel to the square's sides. Explicitly:

$$\frac{\partial u}{\partial n} = (\text{leading order terms}) + \mathrm{e}^{iks} v_+(s) + \mathrm{e}^{-iks} v_-(s) \tag{4.1}$$

where s is the side length, 2π in our case, and $v_\pm(s)$ are non-oscillatory functions, approximated by piecewise polynomials. The oscillatory part is accounted for by the $\mathrm{e}^{\pm iks} = \cos(ks) \pm i\sin(ks)$, so only a small number of piecewise polynomials is needed. These oscillatory basis functions mean that the method is tuned to see the oscillatory nature of the solution, and so doesn't pick up the eigenfunctions of the interior problem, as given by (2.35). The interior eigenfunctions are also oscillatory, but due to either x or y being constant around the square, these eigenfunctions will behave like

$$u(x,y) \approx \sum_{n=0}^{\infty} C_n \cos(\frac{n\pi}{L}x) = \sum_{n=0}^{\infty} C_n \cos(\frac{n}{2}x)$$

on Γ_1 and Γ_3 , or like

$$u(x,y) \approx \sum_{m=0}^{\infty} A_m \cos(\frac{m\pi}{L}y) = \sum_{m=0}^{\infty} A_m \cos(\frac{m}{2}y)$$

on Γ_2 and Γ_4. The hybrid BEM is tuned to approximate

$$\mathrm{e}^{iks} v_+(s) + \mathrm{e}^{-iks} v_-(s) = (\cos(ks) + i\sin(ks))v_+(s) + (\cos(ks) - i\sin(ks))v_-(s)$$

which when considering interior eigenvalues $k = \frac{\pi}{L}\sqrt{n^2+m^2} = \frac{1}{2}\sqrt{n^2+m^2}$ as in (2.33), is tuned to approximate $\cos(ks) = \cos(\frac{1}{2}\sqrt{n^2+m^2}s)$ or $\sin(ks) = \sin(\frac{1}{2}\sqrt{n^2+m^2}s)$. Thus these eigenfunctions will oscillate at different frequencies to $e^{\pm iks}$ if $m, n \neq 0$, and in this case they will not be well approximated by the basis functions. It is only for the case when $m = 0$ or $n = 0$, and k is an integer, that the eigenfunctions may oscillate at the same rate as the solution to the exterior problem.

The functions $v_{\pm}(s)$ are approximated by piecewise polynomials on a graded mesh, specially designed with subintervals spaced so as to equidistribute the approximation error. Since the exterior solution is highly peaked near the corners of the square, the mesh is suitably refined, with larger elements away from the corners and a higher concentration of mesh points around the corners. Thus this should avoid approximating the interior eigenfunctions, even in the case that $m = 0$ or $n = 0$, as there are few mesh points away from the corners. The interval of width one wavelength from the centre is split into N mesh points, and an algorithm then puts $O(\log N)$ points on the rest of the side.

4.2 Numerical Results

The hybrid BEM program was run for $N = 2, 4, 8, 16, 32, 64$ for some of the same values of k as run for the standard BEM in §3.2, as well as for some larger values of k. This enables us to compare whether the hybrid BEM is more effective at finding the exterior solution for those k which are eigenvalues to the interior problem, as given by (2.33) for the cases $\eta = 0$ in which case the standard BEM fails, and for the case $\eta = k$. The program was used to test the importance of the coupling parameter η in finding the unique solution to the exterior problem, rather than the spurious solutions related to the interior problem. When computing errors and relative errors

using the L^2 norm, the exact solution was taken to be that resultant from $\eta = k$, $N = 64$.

Again for graphical output, the four sides of the square were mapped to the X-axis, so that Γ_1 is represented on $0 \leq x \leq 2\pi$, Γ_2 on $2\pi \leq x \leq 4\pi$ Γ_3 on $4\pi \leq x \leq 6\pi$, and Γ_4 on $6\pi \leq x \leq 8\pi$. However, now both the sides in shadow, Γ_1 and Γ_2, and the illuminated sides Γ_3 and Γ_4 have solutions consisting of just the diffracted waves; the behaviour of the reflected wave has been explicitly removed.

Regardless of whether the values of k that are chosen are eigenvalues of the interior problem or not, the hybrid BEM easily converged to the same solutions when using $\eta = 0$ or $\eta = k$, as shown in Figures 4.1 and 4.2. This is further confirmed by Figure 4.3, the L^2 errors when $\eta = 0$ reduce to similar levels as N increases regardless of whether k is an eigenvalue or not. The solution using $\eta = 0$ converged to the exterior solution ($\eta = k$) even for higher, integer values of k as shown in Figure 4.4, despite there being a higher likelihood of approximating the interior solution when $m = 0$ or $n = 0$.

Tables 4.1 and 4.2 show how the relative error decreases at a similar rate regardless of the value of η. It seems to converge to the same level of accuracy for a set N even as k increases. The result for $k = 2.5$ $N = 64$ is slightly unusual, we discuss this later.

Figures 4.5 and 4.6 are log plots, where a logarithmic scale (base 10) is used for the Y-axis. Initially it may appear that the solutions for $\eta = 0$ and $\eta = k$ are different, however, they are essentially the same near corners, where the solution is peaked; the discrepancies between the solutions are on a very small scale. By comparing Figures 4.5 and 4.6 however it is clear that the small differences between the solutions are increasing as $k \to \infty$, for fixed N.

When computing the absolute error for various k, as shown in Figure

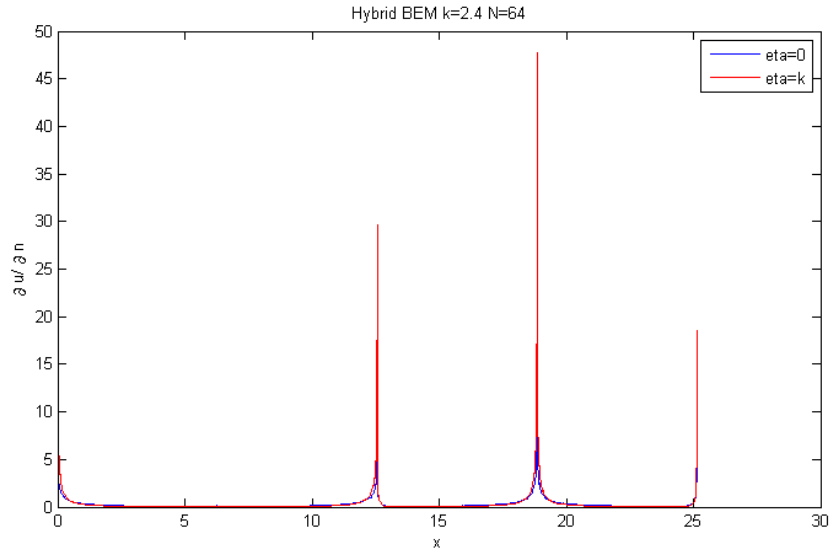

Figure 4.1: k not an Eigenvalue

4.7, the exact solution was taken to be that of $\eta = k$, $N = 64$, and the approximate solution to be that of $\eta = 0$, $N = 64$. The graded mesh seems to have been effective in most cases of removing the peaks in error around the corners of the square.

An interesting case arises when considering low frequencies. As shown in Figure 4.8 the numerical solutions from the hybrid BEM seem to converge to a solution using $\eta = k$ for high N, or using $\eta = 0$ up to a certain number of degrees of freedom, so we can assume this to be the a good approximation to the true solution. However, it seems that for $\eta = 0$ for $N \to \infty$ the solution starts to diverge again. This is most likely because when N is large, there are enough of the piecewise polynomials that approximate the non-oscillatory functions $v_{\pm}(s)$ to approximate the different wavelengths of the interior eigenfunctions. The unusual results for $k = 2.5$, such as the positive EOC, may be explained by this. Figure 4.3 also suggests that the L^2 error may be starting to increase again as N increases for $k = 2.5$.

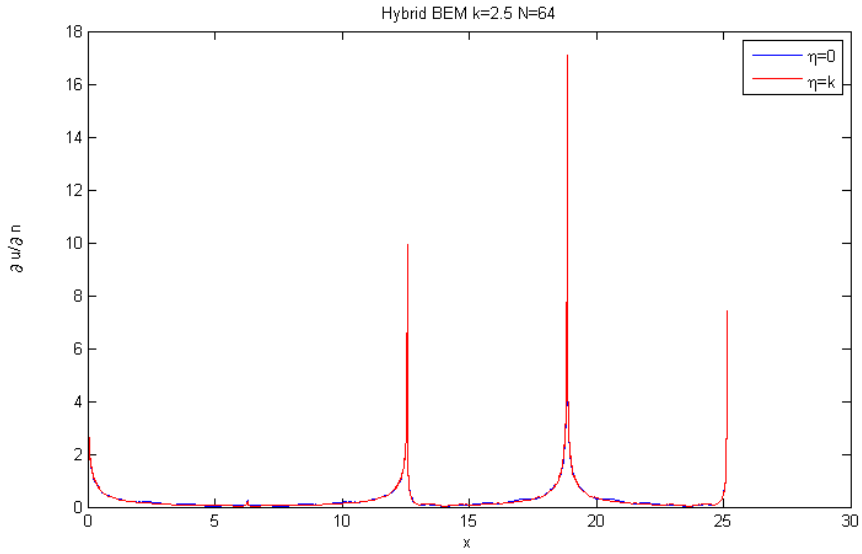

Figure 4.2: k an Eigenvalue

Table 4.3 gives computation time in seconds of how long it took the hybrid code to find a solution using $N = 64$. What is suprising is that regardless of whether the coupled formulation is used or not, there doesn't appear to be a significant difference in computation time; indeed, it occasionally even takes longer using $\eta = 0$. This is because the code computes all functions and then multiplies by η. In future work computations to be multiplied by η could be removed altogether for an $\eta = 0$ version, we would anticipate that this change would reduce the processing time by a factor of 2.

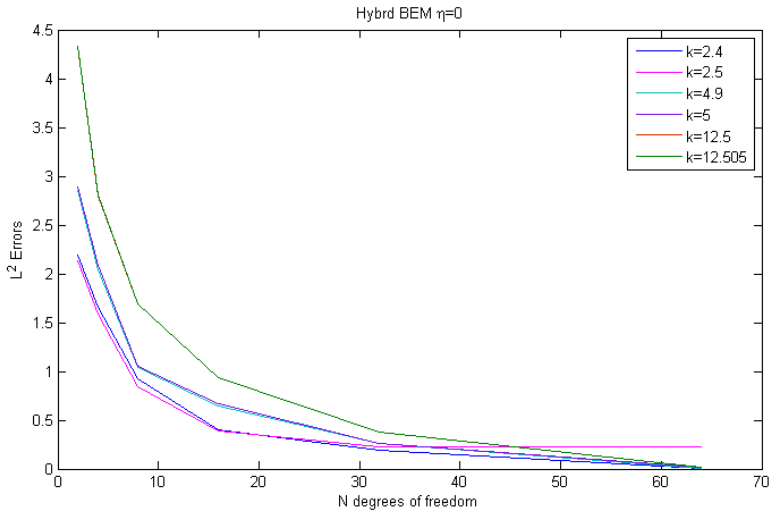

Figure 4.3: L2 Errors against degrees of freedom, for various k

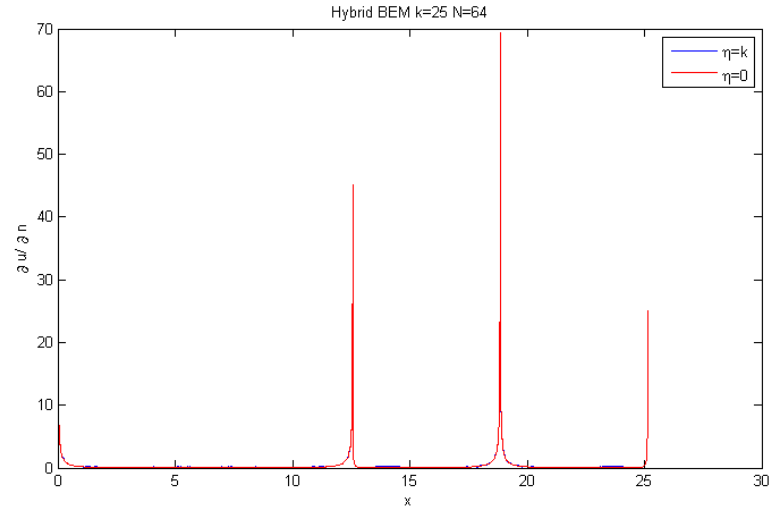

Figure 4.4: k is an Eigenvalue

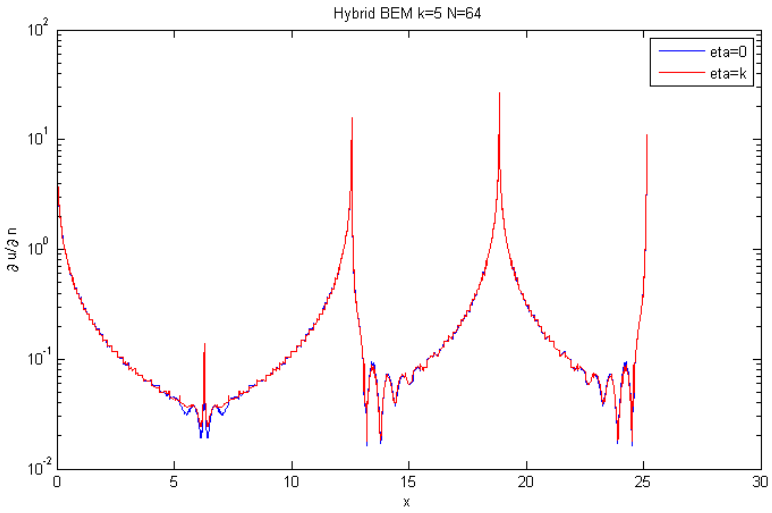

Figure 4.5: k is an Eigenvalue

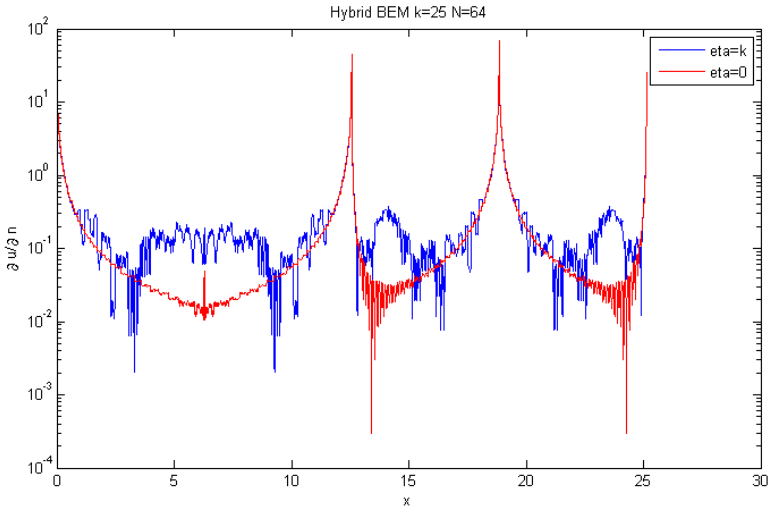

Figure 4.6: k is an Eigenvalue

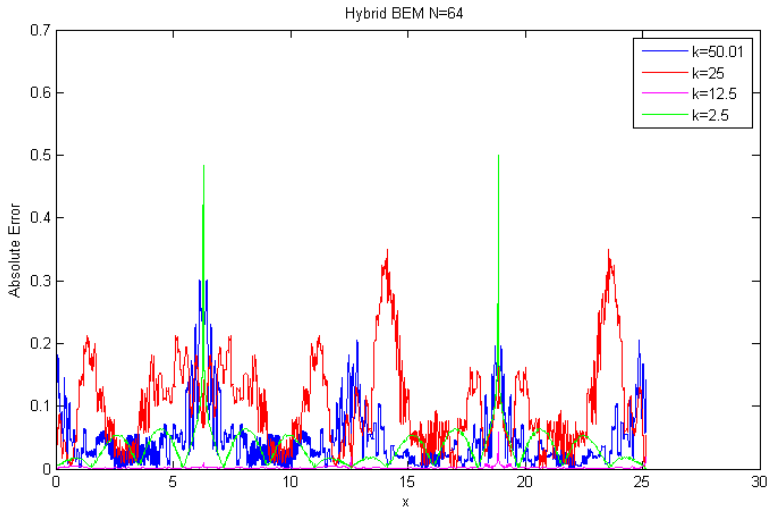

Figure 4.7: Absolute Errors for various k

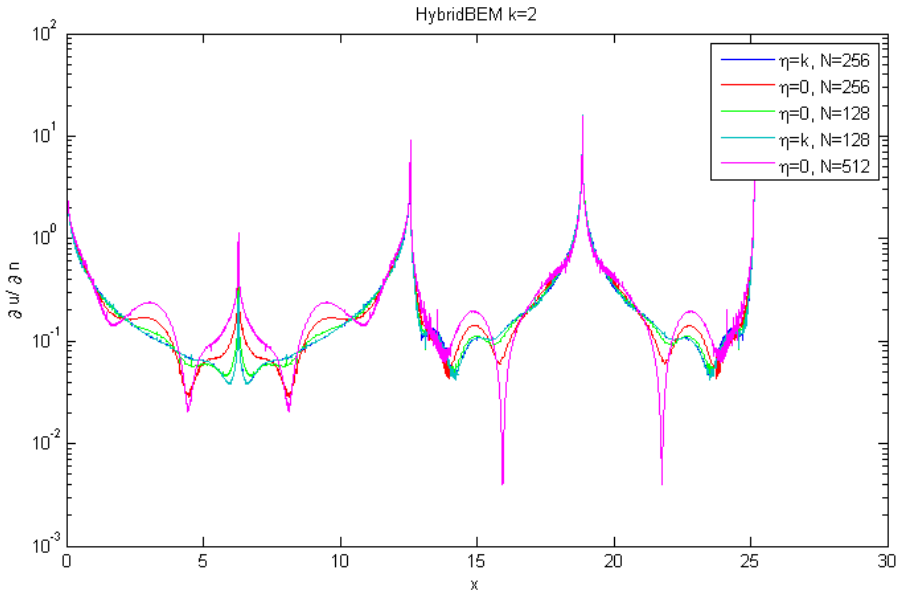

Figure 4.8: Errors arising for a low wavelength $k = 2$ and high N

Table 4.1: Errors and relative L^2 errors for the case that k is an eigenvalue.

		$\eta = 0$			$\eta = k$		
k	N	$\|\|\text{error}\|\|_2$	$\|\|\text{Relative error}\|\|_2$	EOC	$\|\|\text{error}\|\|_2$	$\|\|\text{Relative error}\|\|_2$	EOC
2.5	2	2.1358×10^{0}	6.0377×10^{-1}	-0.4331	2.6999×10^{0}	7.6324×10^{-1}	-0.7660
	4	1.5819×10^{0}	4.4718×10^{-1}	-0.9136	1.5877×10^{0}	4.4882×10^{-1}	-0.9506
	8	8.3975×10^{-1}	2.3739×10^{-1}	-1.1050	8.2151×10^{-1}	2.3223×10^{-1}	-1.1590
	16	3.9039×10^{-1}	1.1036×10^{-1}	-0.7936	3.6790×10^{-1}	1.0400×10^{-1}	-0.9154
	32	2.2523×10^{-1}	6.3669×10^{-2}	0.0183	1.9506×10^{-1}	5.5141×10^{-2}	
	64	2.2810×10^{-1}	6.4481×10^{-2}				
5	2	2.8904×10^{0}	5.9820×10^{-1}	-0.4730	5.4731×10^{0}	1.1327×10^{0}	-1.3546
	4	2.0825×10^{0}	4.3099×10^{-1}	-0.9892	2.1402×10^{0}	4.4293×10^{-1}	-0.5785
	8	1.0491×10^{0}	2.1712×10^{-1}	-0.6597	1.4332×10^{0}	2.9662×10^{-1}	-1.1197
	16	6.6409×10^{-1}	1.3744×10^{-1}	-1.3169	6.5954×10^{-1}	1.3650×10^{-1}	-1.3189
	32	2.6656×10^{-1}	5.5167×10^{-2}	-3.5656	2.6437×10^{-1}	5.4714×10^{-2}	
	64	2.2514×10^{-2}	4.6594×10^{-3}				
12.5	2	4.3275×10^{0}	5.8931×10^{-1}	-0.6273	7.5739×10^{0}	1.0314×10^{0}	-1.3336
	4	2.8016×10^{0}	3.8152×10^{-1}	-0.7285	3.0051×10^{0}	4.0923×10^{-1}	-0.5859
	8	1.6909×10^{0}	2.3026×10^{-1}	-0.8457	2.0022×10^{0}	2.7265×10^{-1}	-1.0542
	16	9.4089×10^{-1}	1.2813×10^{-1}	-1.3152	9.6416×10^{-1}	1.3130×10^{-1}	-1.0704
	32	3.7812×10^{-1}	5.1492×10^{-2}	-4.7594	4.5914×10^{-1}	6.2524×10^{-2}	
	64	1.3961×10^{-2}	1.9012×10^{-3}				
25	2	5.5987×10^{0}	5.6465×10^{-1}	-0.69421	9.8895×10^{0}	9.9739×10^{-1}	-1.0535
	4	3.4603×10^{0}	3.4898×10^{-1}	-0.53202	4.7649×10^{0}	4.8055×10^{-1}	-0.88340
	8	2.3931×10^{0}	2.4135×10^{-1}	-1.0758	2.5829×10^{0}	2.6050×10^{-1}	-0.59577
	16	1.1353×10^{0}	1.1450×10^{-1}	-0.47812	1.7091×10^{0}	1.7237×10^{-1}	-1.0397
	32	8.1505×10^{-1}	8.2201×10^{-2}	-0.38040	8.3138×10^{-1}	8.3848×10^{-2}	
	64	6.2615×10^{-1}	6.3149×10^{-2}				
50.01	2	7.5955×10^{0}	5.7185×10^{-1}	-0.79637	1.3577×10^{1}	1.0222×10^{0}	-1.0897
	4	4.3734×10^{0}	3.2927×10^{-1}	-1.0604	6.3792×10^{0}	4.8028×10^{-1}	-1.1119
	8	2.0971×10^{0}	1.5789×10^{-1}	-0.72881	2.9516×10^{0}	2.2222×10^{-1}	-0.81319
	16	1.2654×10^{0}	9.5271×10^{-2}	-0.79025	1.6798×10^{0}	1.2647×10^{-1}	-0.76657
	32	7.3172×10^{-1}	5.5090×10^{-2}	-1.0936	9.8741×10^{-1}	7.4341×10^{-2}	
	64	3.4288×10^{-1}	2.5815×10^{-2}				

Table 4.2: Errors and relative L^2 errors for the case that k is not an eigenvalue.

		$\eta = 0$			$\eta = k$		
k	N	$\|\|\text{error}\|\|_2$	$\|\|\text{Relative error}\|\|_2$	EOC	$\|\|\text{error}\|\|_2$	$\|\|\text{Relative error}\|\|_2$	EOC
2.4	2	2.1897×10^{0}	6.1962×10^{-1}	-0.39756	2.5422×10^{0}	7.1934×10^{-1}	-0.60605
	4	1.6623×10^{0}	4.7038×10^{-1}	-0.84118	1.6702×10^{0}	4.7260×10^{-1}	-0.85249
	8	9.2791×10^{-1}	2.6256×10^{-1}	-1.2059	9.2498×10^{-1}	2.6174×10^{-1}	-1.2118
	16	4.0222×10^{-1}	1.1382×10^{-1}	-1.1091	3.9934×10^{-1}	1.1300×10^{-1}	-1.0852
	32	1.8647×10^{-1}	5.2765×10^{-2}	-5.6384	1.8823×10^{-1}	5.3261×10^{-2}	
	64	3.7437×10^{-3}	1.0593×10^{-3}				
4.9	2	2.8498×10^{0}	5.9675×10^{-1}	-0.4813	5.6672×10^{0}	1.1867×10^{0}	-1.4335
	4	2.0415×10^{0}	4.2748×10^{-1}	-0.9695	2.0982×10^{0}	4.3936×10^{-1}	-0.6961
	8	1.0426×10^{0}	2.1831×10^{-1}	-0.6860	1.2951×10^{0}	2.7119×10^{-1}	-1.0150
	16	6.4804×10^{-1}	1.3570×10^{-1}	-1.2852	6.4085×10^{-1}	1.3419×10^{-1}	-1.2879
	32	2.6590×10^{-1}	5.5679×10^{-2}	-5.1130	2.6245×10^{-1}	5.4956×10^{-2}	
	64	7.6835×10^{-3}	1.6089×10^{-3}				
12.505	2	4.3281×10^{0}	5.8922×10^{-1}	-0.6270	7.5541×10^{0}	1.0284×10^{0}	-1.3328
	4	2.8026×10^{0}	3.8154×10^{-1}	-0.7289	2.9990×10^{0}	4.0828×10^{-1}	-0.5790
	8	1.6910×10^{0}	2.3021×10^{-1}	-0.8461	2.0077×10^{0}	2.7332×10^{-1}	-1.0595
	16	9.4064×10^{-1}	1.2806×10^{-1}	-1.3141	9.6327×10^{-1}	1.3114×10^{-1}	-1.0735
	32	3.7831×10^{-1}	5.1502×10^{-2}	-4.6524	4.5771×10^{-1}	6.2312×10^{-2}	
	64	1.5043×10^{-2}	2.0479×10^{-3}				

Table 4.3: Processing time in seconds, $N = 64$

k	$\eta = 0$	$\eta = k$
2.4	1459.13949	1457.918595
2.5	1443.757474	1550.433721
4.9	1721.390138	1709.063943
5	1752.560662	1747.952968
12.5	2459.256118	2445.934317
12.505	2455.168543	2491.280168
25	3802.594433	3813.400389
50.01	6924.080258	

Chapter 5

Conclusions and Future Work

5.1 Summary

The main aim of this project was to consider the theory that allows a problem over an infinite exterior domain to be reformulated into a boundary integral formulation over a finite domain. We looked at reformulation using Green's Representation Theorem, and explained the problems of non-uniqueness that arise from this process. Studying in detail the case of a square convex polygon, we showed how these spurious solutions arise. We also aimed to consider methods finding a good approximate solution numerically, even at high wave frequencies, whilst minimising computational expense and avoiding spurious solutions.

We looked at two numerical methods: a standard collocation Boundary Element Method and a hybrid Galerkin BEM as proposed by Langdon and Chandler-Wilde in [1]. By comparing the results of these two methods, it is clear how careful consideration of our desired solution and possible spurious solutions can be used to design a numerical method which avoids the extra computational expense that the theory suggests we will require. The

standard BEM demonstrated how the spurious solutions which relate to the interior problem are easily found. Even when using wavenumbers k that are not eigenvalues of the interior problem, by setting the coupling parameter $\eta = 0$ to avoid the coupled formulation, thus saving computational expense, we still found significant errors. The hybrid BEM incorporated oscillatory basis functions with a graded mesh, based upon detailed study of the exterior solution. These considered improvements did avoid spurious solutions being found even when k was an interior eigenvalue and the coupled formulation was not used, provided a very high level of accuracy was not required. However, the main advantage of using $\eta = 0$ rather than the coupled formulation was expected to be a save in computational time and expense: what resulted in either case turned out to be very similar.

5.2 Further Work

There is a fair amount of scope for further work on this subject. The results we have so far are fairly accurate for lower frequency waves, however the solutions we considered to be exact were those resultant of relatively low N. It would be interesting to allow the hybrid BEM code to run for higher values of N and lower wavenumbers k, and to expand futher into what effect their relationship has on errors. With a deeper understanding of the hybrid code, it may also be relevant to do some error analysis on the numerical results we have produced. It would also have been appropriate to consider how well the hybrid BEM approximates even higher frequencies that would have been considered here, computational time and storage space permitting. As we have found the hybrid BEM to be effective even when using $\eta = 0$, it would be worthwhile to edit the code to make it more cost effective time wise. To do this the code should no longer compute all functions and then multiply them by $\eta = 0$, instead these functions could be removed altogether.

Another aspect that could be considered is to look at the wave scattering problem for various other convex polygons, or even convex curvilinear polygons, to see what effect the graded mesh has in these cases.

Another approach to solving our wave scattering by a square problem would be to consider the assymptotic behaviour around the corners. It has been suggested that by restricting the domain around the corners to a circle, the Helmholtz equation can be solved by separation of variables on polar co-ordinates (r, θ), where r is the radial distance and θ is the external angle. Using this technique, it can be shown that at corners the solution behaves like $C/r^{\frac{1}{2}}$, causing the peaks on the corners. One could design a numerical method that incorporates this, thus avoiding the need for a graded mesh and potentially saving computational time.

Bibliography

[1] S.N. Chandler-Wilde, S. Langdon A Galerkin Boundary Element Method for High Frequency Scattering By Convex Polygons, *SIAM Journal of Numerical Analysis*, **Vol. 45**, 2007, pp. 610-640.

[2] A.J. Burton, G.F. Millar The Application of Integral Equation Methods to the Numerical Solution of some Exterior Boundary-Value Problems, *Procedings of the Royal Society, London*, **A. 323**, 1971, 201-210.

[3] G.F.Roach *Green's Functions: Introductory Theory with Applications*, Van Nostrand Reinhold Company, 1970.

[4] M. Abramowitz, I.A. Stegun *A Handbook of Mathematical Functions*, National Bureau of Standards, 1968.

[5] D. Colton, R. Kress *Inverse Accoustic and Electromagnetic Scattering Theory*, Springer-Verlag, 1998.

[6] Ian H. Sloan *Theory and Numerics of ODE's and PDE's*, Editors: Ainsworth, Levesley, Light, and Marletta. Oxford Science Publications, 1994.

[7] `http://www.personal.reading.ac.uk/~sms03snc/fe_bem_notes_sncw.pdf`, Boundary element methods for acoustics, (last checked on 18.08.2009).